Optimization of the distance between source and substrate for device-grade SnS films grown by the thermal evaporation technique

2007 J. Phys.: Condens. Matter 19 306003

(http://iopscience.iop.org/0953-8984/19/30/306003)

IOP PUBLISHING JOURNAL OF PHYSICS: CONDENSED MATTER

J. Phys.: Condens. Matter **19** (2007) 306003 (12pp) doi:10.1088/0953-8984/19/30/306003

Optimization of the distance between source and substrate for device-grade SnS films grown by the thermal evaporation technique

M Devika[1], N Koteeswara Reddy[2,6], D Sreekantha Reddy[1], S Venkatramana Reddy[1], K Ramesh[2], E S R Gopal[2], K R Gunasekhar[3], V Ganesan[4] and Y B Hahn[5]

[1] Department of Physics, Sri Venkateswara University, Tirupati-517 502, India
[2] Department of Physics, Indian Institute of Science, Bangalore-560 012, India
[3] Department of Instrumentation, Indian Institute of Science, Bangalore-560 012, India
[4] CSR, Indore Centre, Indore-452017, India
[5] School of Semiconductor and Chemical Engineering, BK21 Center for Future Energy Materials and Devices, Chonbuk National University, Jeonju-561756, Korea

E-mail: dr_nkreddy@rediffmail.com

Received 27 May 2007, in final form 14 June 2007
Published 11 July 2007
Online at stacks.iop.org/JPhysCM/19/306003

Abstract

Tin monosulfide (SnS) films with varying distance between the source and substrate (DSS) were prepared by the thermal evaporation technique at a temperature of 300 °C to investigate the effect of the DSS on the physical properties. The physical properties of the as-deposited films are strongly influenced by the variation of DSS. The thickness, Sn to S at.% ratio, grain size, and root mean square (rms) roughness of the films decreased with the increase of DSS. The films grown at DSS = 10 and 15 cm exhibited nearly single-crystalline nature with low electrical resistivity. From Hall-effect measurements, it is observed that the films grown at DSS $\leqslant$ 15 cm have p-type conduction and the films grown at higher distances have n-type conduction due to the variation of the Sn/S ratio. The films grown at DSS = 15 cm showed higher optical band gap of 1.36 eV as compared with the films grown at other distances. The effect of the DSS on the physical properties of SnS films is discussed and reported.

(Some figures in this article are in colour only in the electronic version)

[6] Author to whom any correspondence should be addressedPresent address: SCET, Chonbuk National University, Jeonju-561756, Korea.

1. Introduction

Tin monosulfide (SnS), a narrow band gap material (1.36 eV [1]), has been attracting interest due to its properties that are favourable for the fabrication of optoelectronic devices. In particular, it is a potential candidate for the development of photovoltaic devices [2–5], photodetectors [6], solid-state lubricants [7], near-infrared detectors [8], anode material in lithium micro-batteries [9], and commercial semiconductor sensors in environmental industrial and biomedical monitoring [10]. In this regard, a large number of investigations have been carried out to synthesize device-grade SnS films and test their suitability for different applications. Recently, Avellaneda *et al* [11] prepared chemically deposited SnS film-based heterostructures and studied their performance by annealing them at different temperatures. Low-resistive SnS films (16 Ω cm) with p-type as well as n-type conduction have been prepared by Cheng *et al* [12] using electrodeposition on indium tin oxide (ITO) substrates. By using an SnS-based nanocomposite thin-film electrode, Li *et al* [13] prepared lithium ion batteries and observed an excellent cycling stability of the device. Sánchez-Juárez *et al* [14] prepared SnS/SnS_2 heterostructures using plasma-enhanced chemical vapour deposition and the photovoltaic effect was studied.

In our earlier studies, we investigated the influence of substrate temperature [1], thickness [15], substrate surface [16], annealing [17] and Ag doping [18] on the physical properties of SnS films grown by the thermal evaporation technique. One of the other important deposition parameters, the distance between the source and substrate (DSS), has to be optimized to obtain good-quality SnS films. To the best of our knowledge, there is no report on the influence of DSS on the physical properties of SnS films. Hence, there deserves to be an investigation of the above effect on the SnS films. In this paper, we report systematic investigations on the influence of the DSS on the physical properties of SnS films grown by the thermal evaporation technique.

2. Experimental procedure

SnS films were deposited using the thermal evaporation system on Corning 7059 glass substrates. The depositions were carried out at various distances between the source and substrates (5, 10, 15, 20, and 25 cm) in a vacuum of $\sim 10^{-6}$ Torr. The other parameters such as substrate temperature (300 °C), rate of deposition (2 Å s^{-1}) and weight of the source material (50 mg) were kept as constant. Highly pure (4N) SnS compound was used as the source material and evaporated using a molybdenum boat by applying a constant voltage of 30 V with a current of 65 A. A 1 kW radiant heater was used to heat the substrates and a temperature controller was employed to control the substrate temperature with an accuracy of ±2 °C.

The thickness (roughly) of the as-deposited films was estimated by gravimetric method using a Sartorius Research microbalance (Model: R 200D) system. The elemental composition of the films was examined using energy dispersive analysis of x-rays (EDAX) system attached to a scanning electron microscope (SEM; model JSM-840 A). The structural properties were studied using the x-ray diffraction (XRD) spectra collected from a x-ray diffractometer (Philips X'Pert Pro). The surface topology and morphology of the SnS films were examined using the SEM and an atomic force microscope (AFM; Digital Instrument Nanoscope-E) at room temperature. In order to study the electrical properties of the SnS films, Hall-effect measurements were carried out at room temperature. The temperature-dependent resistance studies were also carried out using a high-resistance Keithley electrometer (model 6517A) in the temperature range 20–200 °C under a vacuum of 10^{-2} Torr. The temperature was controlled using a temperature controller with an accuracy of ±2 °C. Transmittance spectra of the SnS

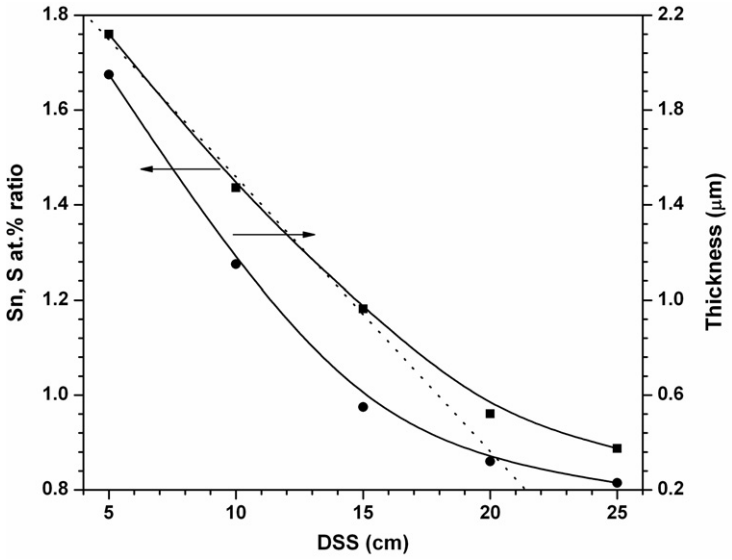

Figure 1. Variation of Sn to S at.% ratio and thickness of SnS films with DSS.

films were recorded using a Fourier transform infra-red (FTIR) spectrophotometer (Bruker IFS 66V/S) in the wavelength range 500–2500 nm, with incident light perpendicular to the cleavage plane of the film.

3. Results and discussions

The physical properties of SnS films are strongly influenced by the DSS. The colour of the films changed from brownish black to greenish yellow with the increase of the DSS. While increasing the DSS the adherence of the films also increased. The films deposited at lower DSS exhibited loosely packed ashy surfaces, and with increasing DSS the adherence of the films increased. The thickness of the films decreased with the increase of the DSS, as shown in figure 1. This variation is attributed to the availability of evaporated atoms at the hot substrate. In general, the number of evaporated atoms reaching the hot substrate at lower distances is high as compared to higher distances, since the rate of impingement of the evaporated atoms on the hot substrate is directly proportional to the source power and vacuum in the system and indirectly proportional to the DSS [19]. Here, the source power and vacuum in the system were constant, therefore the rate of deposition of atoms on the hot substrate strongly depends on the DSS.

3.1. Composition analysis

The composition analysis of the SnS films showed that the tin and sulfur content in the films gradually varied with the increase of DSS. The obtained composition of the SnS films is given in table 1. Figure 1 shows the variation of the Sn to S at.% ratio with DSS. It reveals that the films grown at lower distances are sulfur deficient as compared to the films grown at higher distances. It also shows a deviation in the variation of Sn to S at.% ratio from its linear trend at DSS $>$ 15 cm. The variation of Sn to S at.% ratio with DSS can be explained with the help of the kinetic energy (KE) of the evaporated atoms on the hot substrate. At lower distances

Table 1. The observed elemental composition of SnS films and their lattice parameters.

			Lattice parameters			
			Observed (nm)			
DSS (cm)	Sn (at.%)	S (at.%)	a	b	c	Standard (nm)
5	63.77	36.23	0.433	1.119	0.398	
10	58.95	41.05	0.433	1.119	0.398	$a = 0.433$
15	54.17	45.83	0.433	1.123	0.399	$b = 1.119$
20	49.00	51.00	0.433	1.124	0.397	$c = 0.398$
25	47.02	52.98	0.432	1.124	0.398	

(<10 cm), the KE of the deposited atoms, particularly for sulfur atoms, is high due to their high vapour pressure. These sulfur particles scatter from the hot substrate and cause the films to be sulfur deficient, resulting in a high value of the Sn to S at.% ratio. However, the low value of the Sn to S at.% ratio of the films grown at higher distances (>15 cm) might be due to the low KE of the heavy Sn atoms as well as the considerable decrease of scattering of S atoms. This causes the films to be rich in sulfur content at higher distances and results in a low value of the Sn to S at.% ratio.

3.2. Structural studies

Structural analysis of the as-deposited films showed that the variation of DSS strongly affects the growth and size of crystallites of the films. The XRD spectra of SnS films deposited at three distances of 5, 15, and 25 cm are shown in figure 2. The films deposited at lower (DSS $\leqslant$ 10 cm) and higher (DSS $\geqslant$ 20 cm) distances exhibited polycrystalline nature. These polycrystalline films exhibited peaks at $2\theta = 22.01°$, 25.96°, 27.34°, 30.44°, 31.56°, 31.86°, 38.97°, and 66.64°. The evaluated d-spacing values and lattice parameters (given in table 1) of the films nearly match the JCPDS data of SnS (card no. 39-0354). Hence, the above peaks belong to (110), (120), (021), (101), (111), (040), (131), and (080) reflections, respectively. However, the films deposited at DSS = 15 cm showed only two peaks, at 31.86° and 66.64°, that correspond to (040) and (080) planes, respectively. This reveals that the films grown at around DSS = 15 cm are nearly single crystalline in nature. Therefore, the crystallites in the SnS films were crystallized orthorhombically. In this study, however, we could not observe any other tin sulphide binary phases like SnS_2 and Sn_2S_3. It is important to point out that the as-deposited SnS films grown at all distances, even though they have different thicknesses, exhibited the (040) peak as a dominant peak. This indicates that most of the crystallites are grown along the [010] direction. However, it is observed in our earlier studies that the films grown at below 0.75 μm thickness exhibited (111) peak as a dominant while at thickness $\geqslant$0.75 μm showed (040) as well as (111) peaks as dominant [15]. This difference in preferred orientation of SnS films is attributed to the rate of evaporation of the source material.

The average grain size of the films, evaluated using Scherrer's formula, decreased from 217 to 117 nm with the increase of DSS as shown in figure 3. However, on increasing the DSS, the degree of preferred orientation (DPO) of the films, DPO = I(040)/I(080), increased. The variation of DPO with DSS is also shown in figure 3. The decrease of average grain size of the films with the DSS is mainly attributed to the variation of adatom mobility of evaporated atoms. At lower distances, because of the high mobility of deposited atoms, the coalescence of the nuclides increases and this results in the grain size increasing to larger values. On increasing the DSS, the coalescence of the nuclides decreased due to the decrease of adatom mobility. This

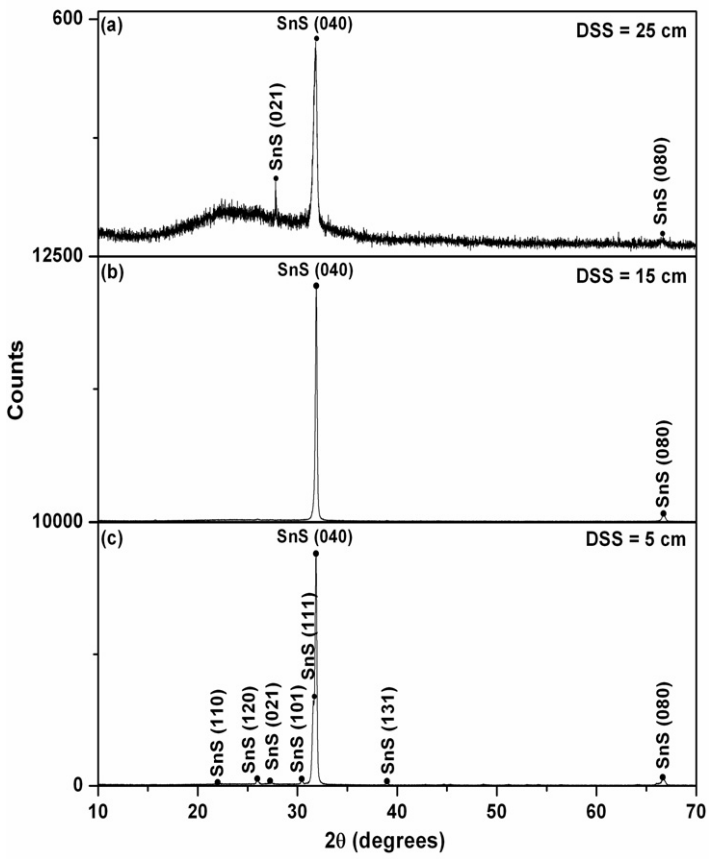

Figure 2. XRD spectra of SnS films grown at three typical distances.

might be a reason for low grain size at higher distances. The exponential increase of DPO with DSS depicts an improvement in the crystallinity of the SnS films.

3.3. Surface analysis

Figure 4 shows the SEM pictures of SnS films grown at different distances: (a) 5, (b) 15, and (c) 25 cm, respectively. It can be seen that the surface structure of the films drastically changed with the change of DSS. The SnS films grown at lower distances exhibited quite large granular structure. These granules are grown randomly with irregular shapes and sizes. It also appears that the grown granules are loosely packed together and form a highly rough surface. On increasing the DSS, the granular size as well as roughness of the films decreased. These changes in the surface structure of the films were clearly observed in the AFM analysis. The AFM pictures of SnS films, grown at DSS $=$ 5, 15, and 25 cm, recorded over an area of $1 \times 1\ \mu m^2$, are also shown in figure 4. The AFM studies revealed that the granules on the films surface have a smooth surface and are surrounded by deep voids. With the increase of DSS, the depth of voids decreased and the number of granules on the surface of the films increased. The average grain size of the films, evaluated using a standard statistical averaging technique, decreased with DSS, and these values nearly match the data obtained from the XRD studies.

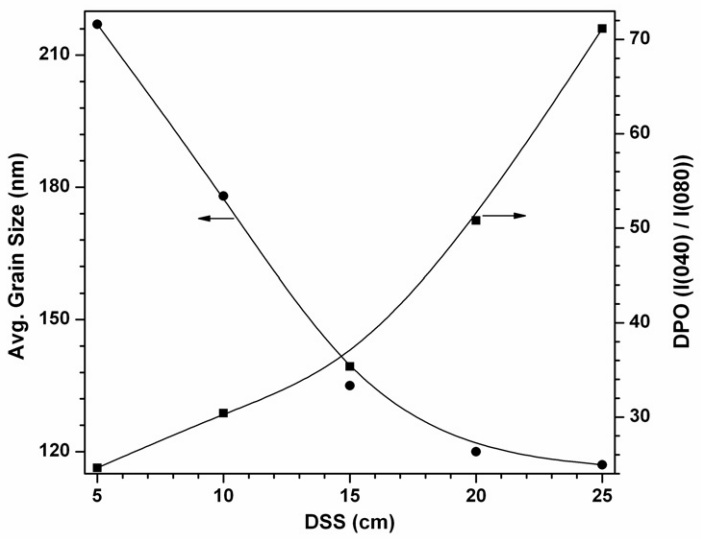

Figure 3. Variation of average grain size and DPO of SnS films with DSS.

The rms roughness of the films, extracted from AFM pictures, also decreased from 72 to 8 nm with the increase of DSS, as shown in figure 5.

3.4. Electrical properties

The electrical resistivity, carrier density, and Hall mobility of the SnS films were evaluated from Hall-effect measurements. Besides these, from the above measurements it is observed that the films grown at DSS $>$ 15 cm exhibit n-type conduction and however, the films grown at DSS $\leqslant$ 15 cm exhibit p-type conduction. The n-type conduction in SnS films is due to excess sulfur content in the layers grown at DSS $>$ 15 cm (Sn/S $<$ 1). The evaluated resistivity of the films varied between 11 and 55 Ω cm with the increase of DSS, as shown in figure 6. The films deposited at 10 cm $>$ DSS $>$ 15 cm exhibited high electrical resistivity ($>$30 Ω cm) as compared to the films grown at a DSS between 10 and 15 cm. In general, the resistivity of the films depends on thickness, grain size, composition, defects, and/or surface roughness of the films. In the present study, the films grown at DSS $=$ 5 cm showed slightly high resistivity, even though the thickness, Sn to S at.% ratio, and grain sizes are high, as compared to the films grown at 10 cm. Above this distance, the film resistivity increased with the increase of DSS due to the decrease of film thickness, Sn to S at.% ratio, and/or grain size. Interestingly, the films grown at DSS $=$ 10 and 15 cm exhibited low resistivity ($\sim$11.5 Ω cm). However, this value is slightly smaller than the value ($\sim$30 Ω cm) reported in our earlier studies on SnS films grown at DSS $=$ 14 cm [1]. This variation is mainly attributed to the rate of evaporation of the source material. The variation of carrier density and Hall mobility of SnS films is shown in figure 7. It can be seen that the density of carriers in the films initially increased with DSS and reached a maximum value of 3.1×10^{16} cm^{-3} at DSS $=$ 10 cm and then decreased. The films formed in the DSS range between 10 and 15 cm showed a net carrier density of the order of 10^{16} cm^{-3}, which is lower than the reported data on SnS single crystals [20, 21]. On the other hand, the Hall mobility of the carriers decreased rapidly with DSS and reached a minimum value of 18 cm^2 V^{-1} s^{-1} at a DSS of 10 cm and then increased. The peculiar behaviour of SnS films grown at DSS $=$ 5 cm might be due to the presence of unreacted deposited species on the

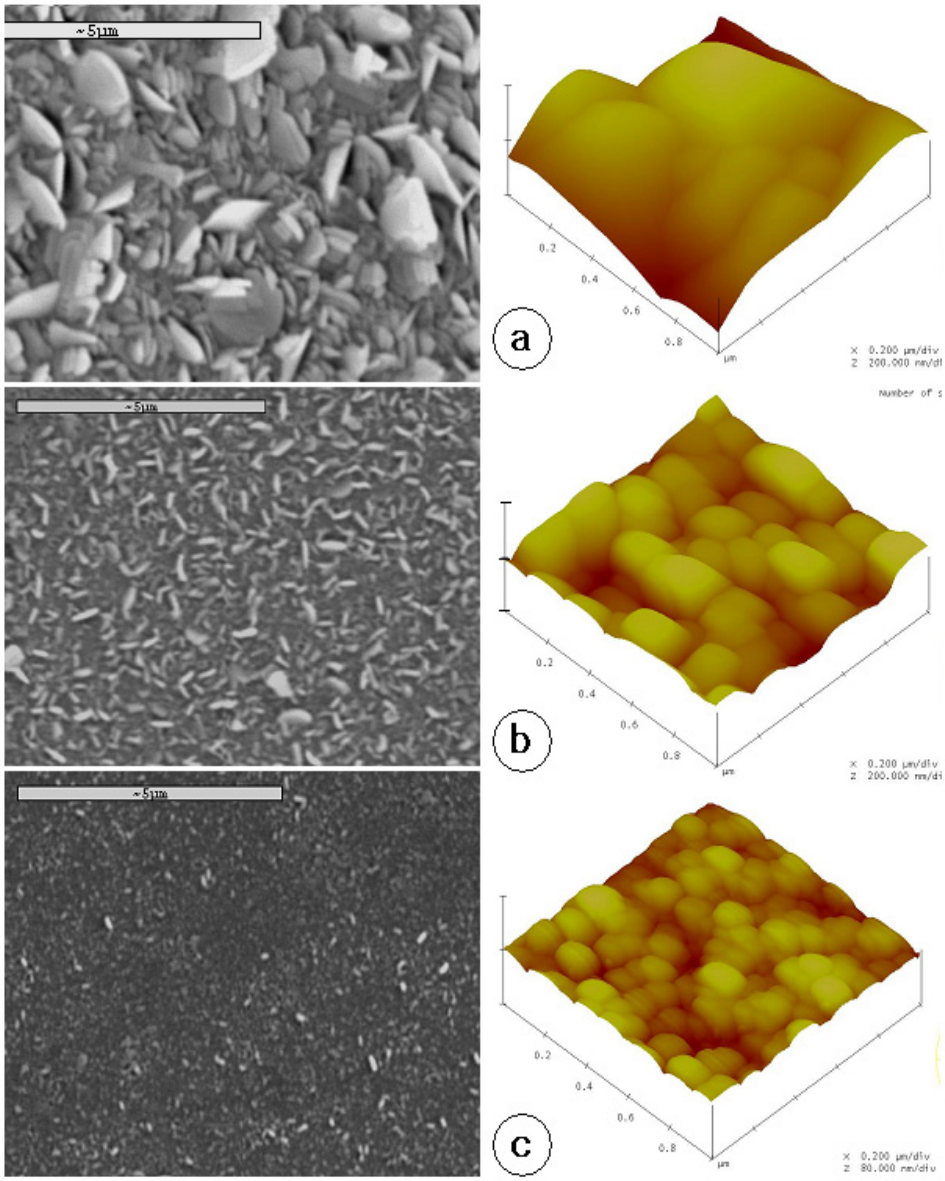

Figure 4. SEM and AFM pictures of SnS films grown at DSS = 5, 15, and 25 cm respectively.

surface of the films. A drastic variation in carrier density, Hall mobility and also in resistivity of the films grown at DSS $>$ 15 cm may be an indication of the change of conductivity from p-type to n-type. This type of behaviour was observed in SnS films grown at different substrate temperatures using the spray pyrolysis method [22].

The activation energy of the SnS films has been evaluated using the Arrhenius equation, $\sigma = \sigma_o \exp(-\Delta E/kT)$, where σ is the conductivity, σ_o the proportionality constant, k Boltzmann's constant, and T the absolute temperature. The temperature-dependent electrical resistivity (ρ) was measured in the temperature (T) range 20–200 °C. The activation energy

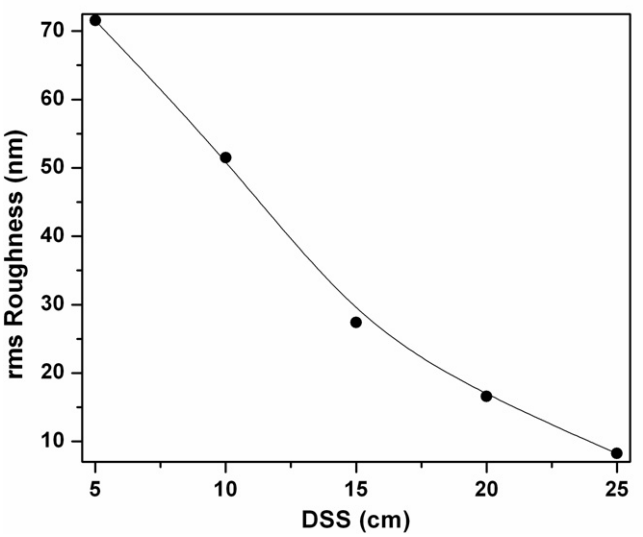

Figure 5. Variation of rms roughness of SnS films with DSS.

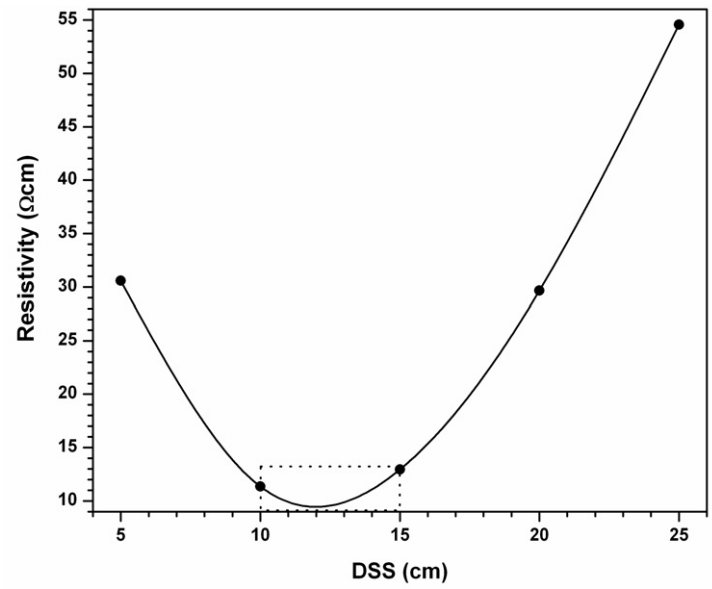

Figure 6. Variation of electrical resistivity of SnS films with DSS.

of the SnS films was calculated from the slope of the semi-log of the normalized conductivity ($\ln(n(\sigma))$) versus $1/T$ plots. A slant variation is observed in the conductivity with the increase of temperature that represents extrinsic behaviour of the SnS films. Here, the conductivity varies due to the ionized acceptors or donors liberated from the impurity atoms. In our earlier studies, a similar trend was observed in $\ln(n(\sigma))$ versus $1/T$ plots of SnS films grown at different thicknesses [15]. The variation of activation energy of SnS films with DSS is shown in figure 8. It can be seen that the films grown at DSS $=$ 10 and 15 cm showed low

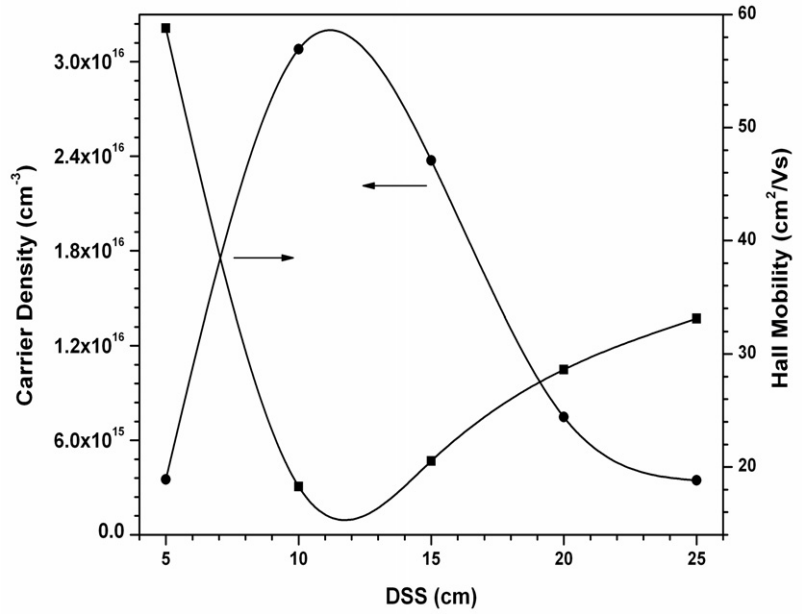

Figure 7. Variation of carrier density and Hall mobility of SnS films with DSS.

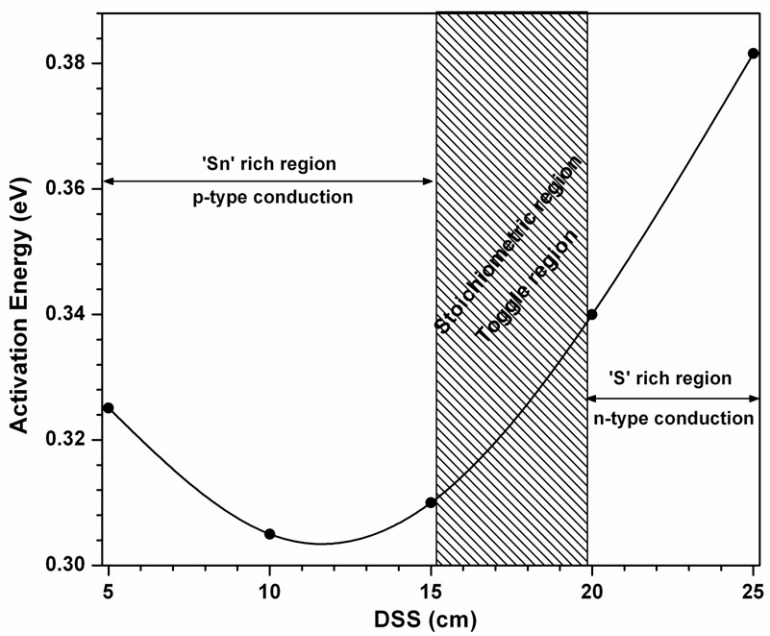

Figure 8. Variation of activation energy of SnS films with DSS.

activation energy values as compared to the films grown at other distances. This variation in activation energy of SnS films with the DSS can be understood with the help of thickness and stoichiometry of the films. In general, the nearly stoichiometric and/or thicker films exhibit

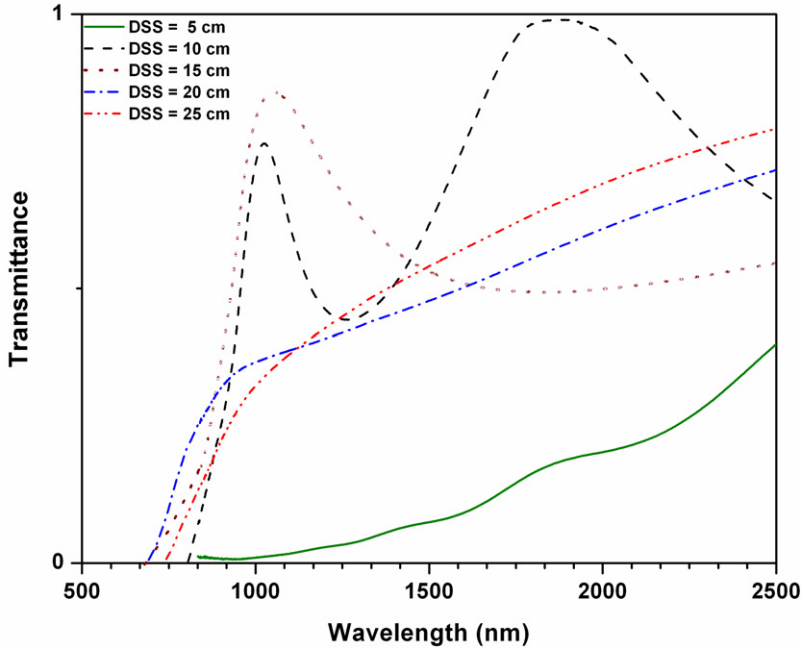

Figure 9. Transmittance versus wavelength plots of SnS films grown at different distances.

lower activation energy than the non-stoichiometric and/or thinner films [15]. Hence, the high activation energy of SnS films grown at DSS $<$ 10 cm, even though their thickness is high, is mainly attributed to their non-stoichiometric nature. However, the high activation energy of the films grown at DSS $>$ 15 cm is due to both factors: thickness as well as non-stoichiometry. This strongly supports the results observed in Hall-effect measurements.

3.5. Optical properties

The optical behaviour of SnS films deposited at various distances has been studied with the help of optical transmittance (T) versus wavelength spectra at room temperature, as shown in figure 9. The SnS films grown at DSS $=$ 10 and 15 cm exhibited interference peaks. However, the films grown at 5 cm showed very low transmittance with low-magnitude interference peaks due to either high absorption and/or reflectance, whereas the films grown at DSS $\geqslant$ 20 cm did not exhibit interference peaks due to low film thickness [15]. It can also be seen that the films grown at all distances except DSS $=$ 5 cm showed a sharp fall in transmittance. Below the fundamental absorption edge, i.e., at lower wavelengths, the absorption coefficient of the films was calculated using the equation $\alpha = \ln(1/T)/t$. From α versus photon energy (E) plots it is observed that the SnS films are direct band gap films, since α increases sharply with photon energy. The optical band gap of the as-deposited films was evaluated from the plots of $(\alpha h\nu)^2$ versus E by extrapolating the linear part of the line to $(\alpha h\nu)^2 = 0$. $(\alpha h\nu)^2$ versus E plots of SnS films grown at DSS $=$ 5, 15 and 25 cm are shown in figure 10. The evaluated optical band gap of SnS films varied between 0.94 and 1.36 eV with DSS, as shown in figure 11. Here, the films grown at DSS $=$ 5 cm exhibited very low band gap of 0.94 eV due to high thickness, tin content, and grain size. Figure 11 reveals that the optical band gap of the films increased with the increase of DSS up to 15 cm and reached a maximum value of 1.36 eV. With further

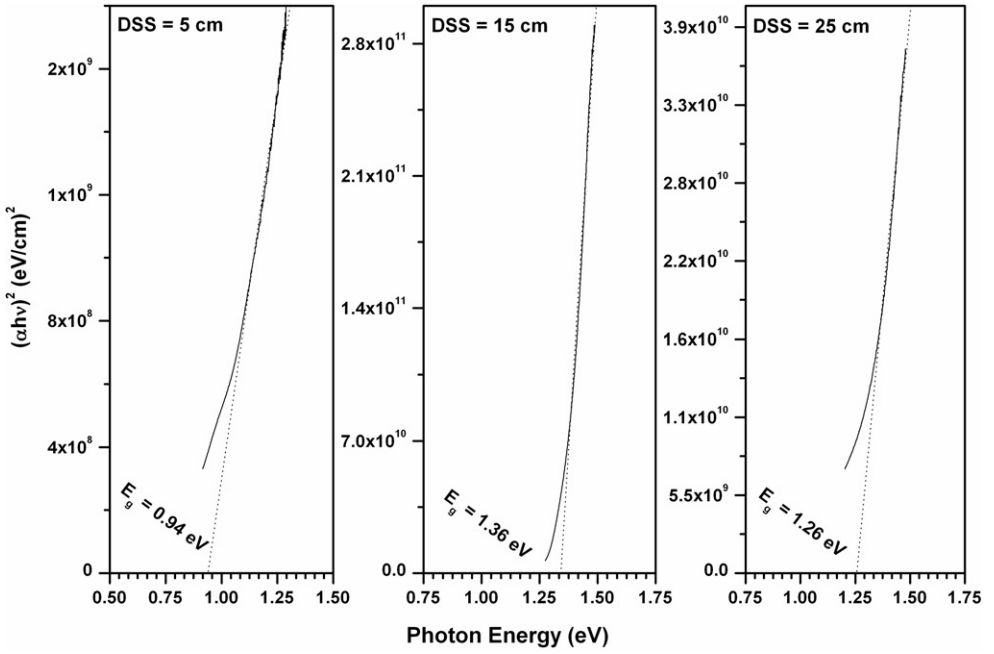

Figure 10. $(\alpha h\nu)^2$ versus photon energy plots of SnS films grown at DSS = 5, 15, and 25 cm respectively.

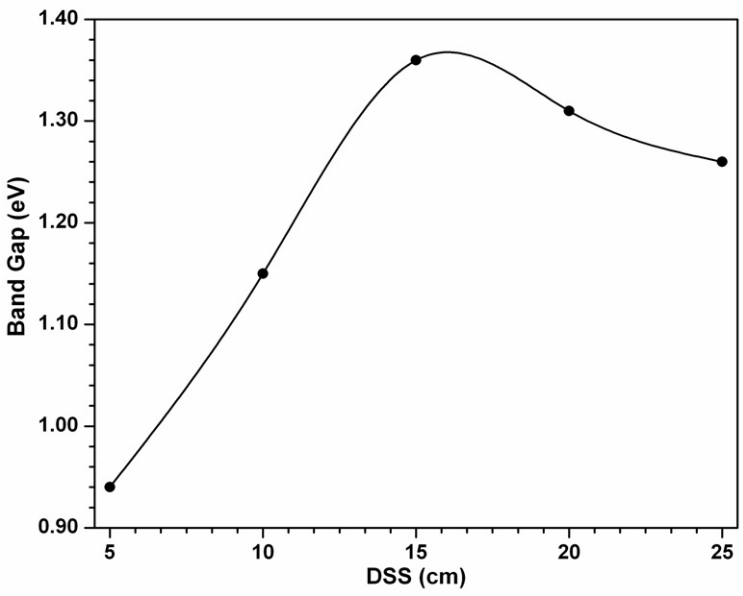

Figure 11. Variation of optical band gap of SnS films with DSS.

increase of DSS, even though the sulfur content in the films increases, the optical band gap decreases. The initial increase of optical band gap with DSS is due to the decrease of film

thickness and increase of sulfur content. A decrease of band gap at higher distances is due to a drastic increase in the DPO of the films.

4. Conclusions

SnS films grown on glass substrates at various distances between the source and substrate exhibited interesting physical properties. The as-deposited films showed single SnS phase and their Sn to S at.% ratio, grain size, and rms roughness decreased with the increase of DSS. However, the films grown at DSS = 10 and 15 cm showed lower electrical resistivity and higher Hall mobility than the films grown at other distances. Interestingly, the Sn-rich films exhibited p-type conductivity whereas S-rich films showed n-type conductivity. The evaluated optical band gap of the SnS films initially increased with DSS up to 15 cm due to a decrease of thickness, grain size, and also an increase of sulfur content. Above 15 cm, the band gap decreased because of a drastic increase in the DPO of the films. Hence, it can be concluded that the films grown between 10 and 15 cm have shown favourable properties for the fabrication of SnS-based devices. Therefore, to obtain device-grade SnS films using the thermal evaporation technique one should deposit the films by keeping the DSS value between 10 and 15 cm.

Acknowledgment

The authors wish to acknowledge the financial support from CSIR, New Delhi, India.

References

[1] Devika M, Ramakrishna Reddy K T, Koteeswara Reddy N, Ramesh K, Ganesan R, Gopal E S R and Gunasekhar K R 2006 *J. Appl. Phys.* **100** 023518
[2] Singh J P and Bedi R K 1991 *Thin Solid Films* **199** 9
[3] Ramakrishna Reddy K T, Koteeswara Reddy N and Miles R W 2006 *Solar Energy Mater. Sol. Cells* **90** 3041
[4] Loferski J J 1956 *J. Appl. Phys.* **27** 777
[5] Gunasekaran M and Ichimura M 2007 *Sol. Energy Mater. Sol. Cells* **91** 774
[6] Johnson J B, Jones H, Latham B S, Parker J D, Engelken R D and Barber C 1999 *Semicond. Sci. Technol.* **14** 501
[7] Kana A T, Hibbert T G, Mahon M F, Molloy K C, Parkin I P and Price L S 2001 *Polyhedron* **20** 2989
[8] Pramanik P, Basu P K and Biswas S 1987 *Thin Solid Films* **150** 269
[9] Valiukonis G, Guseinova D A, Keivaitb G and Sileika A 1990 *Phys. Status Solidi* b **135** 299
[10] Jiang T, Ozin G A, Verma A and Bedard R L 1998 *J. Mater. Chem.* **8** 1649
[11] Avellaneda D, Delgado G, Nair M T S and Nair P K 2007 *Thin Solid Films* **515** 5771
[12] Cheng S, Chen Y, He Y and Chen G 2007 *Mater. Lett.* **61** 1408
[13] Li Y, Tu J P, Huang X H, Wu H M and Yuan Y F 2007 *Electrochem. Commun.* **9** 49
[14] Sánchez-Juárez A, Tiburcio-Silver A and Ortiz A 2005 *Thin Solid Films* **480/481** 452
[15] Devika M, Koteeswara Reddy N, Ramesh K, Ganesan R, Gunasekhar K R, Gopal E S R and Ramakrishna Reddy K T 2007 *J. Electrochem. Soc.* **154** H67
[16] Devika M, Koteeswara Reddy N, Ramesh K, Sumana H R, Gunasekhar K R, Gopal E S R and Ramakrishna Reddy K T 2006 *Semicond. Sci. Technol.* **21** 1495
[17] Devika M, Koteeswara Reddy N, Ramesh K, Gunasekhar K R, Gopal E S R and Ramakrishna Reddy K T 2006 *Semicond. Sci. Technol.* **21** 1125
[18] Devika M, Koteeswara Reddy N, Ramesh K, Gunasekhar K R, Gopal E S R and Ramakrishna Reddy K T 2006 *J. Electrochem. Soc.* **153** G727
[19] Maissel L I and Glang R 1970 *Hand Book of Thin Film Technology* (New York: McGraw-Hill) pp 1–36
[20] Trbojevic D, Nikolic P M, Perovic B and Cvekic V 1981 *Appl. Phys. Lett.* **38** 362
[21] Chamberlain J M, Nikolic P M, Merdan M and Mihailovic P 1976 *J. Phys. C: Solid State Phys.* **9** L637
[22] Koteeswara Reddy N and Ramakrishna Reddy K T 2005 *Solid-State Electron.* **49** 902